A model for estimating Ag-MAR flooding duration based on crop tolerance, root depth, and soil texture data

Yonatan Ganot [*], Helen E. Dahlke

Land, Air and Water Resources, University of California, Davis, CA, USA

A B S T R A C T

Agricultural Managed Aquifer Recharge (Ag-MAR) is an emerging MAR technique that uses agricultural fields as percolation basins to recharge the underlying aquifers. Ag-MAR can be a beneficial solution for storing excess surface water, however, if not managed properly it can potentially harm the soil and crops planted on the field at the time of recharge, ultimately leading to yield loss. Root zone residence time (RZRT), defined as the duration that the root-zone can remain saturated (or nearly saturated) during Ag-MAR without crop damage, is a key factor in Ag-MAR since extended periods of saturation in the root-zone can damage crops. Here we propose a simple RZRT model for estimating a safe Ag-MAR flooding duration based on hydraulic parameters deduced from soil texture, crop tolerance to saturation, effective root depth, and critical soil water content, which is the point where soil re-aeration occurs during drainage. We tested the model with different hydraulic parameter sets and compared the results to observed data and HYDRUS simulations. Using fitted and unfitted hydraulic parameters the average error of the predicted Ag-MAR flooding duration was less than 5 h, and up to a few days, respectively. Consequently, for crops with low flooding-tolerance, the model should be used with caution, but for more tolerant crops, the model provides reasonable predictions. The model also provides a first approximation of the possible amount of water that can be applied during an Ag-MAR event. Based on the RZRT model, we evaluated the Ag-MAR potential of various crops and effective root depths for each of the USDA soil texture classes. A spreadsheet containing the RZRT model including hydraulic parameters, and crop properties is publicly available and can be used as a learning tool or to estimate Ag-MAR flooding duration for different soils. The proposed model can be easily integrated into Ag-MAR assessment tools.

1. Introduction

Agricultural managed aquifer recharge (Ag-MAR) is a recharge technique for groundwater replenishment, in which farmland is flooded during the winter using excess surface water in order to recharge the underlying aquifer (Bachand et al., 2014; Dahlke et al., 2018b; Kocis and Dahlke, 2017). In California, for example, Ag-MAR is currently being implemented as part of the efforts to mitigate California's chronic groundwater overdraft (Faunt et al., 2016; Harter, 2015; SGMA, https://water.ca.gov/programs/groundwater-management/sgma-groundwater-management).

Ag-MAR poses several risks for agricultural fields and groundwater that may influence its future adoption. This includes crop tolerance to flooding, soil aeration, biogeochemical transformations, long-term impact on soil texture, leaching of pesticides and fertilizers to groundwater, and potential greenhouse gas emissions. Some of these issues

have been addressed in recent studies of Ag-MAR, including soil suitability guidelines (O'Geen et al., 2015), nitrate leaching to groundwater (Bachand et al., 2014; Bastani and Harter, 2019; Waterhouse et al., 2020), crop suitability (Dahlke et al., 2018a) and soil aeration (Bachand et al., 2019; Ganot and Dahlke, 2021). In the current study, we focused solely on the question of "how long can water be applied for Ag-MAR with minimal crop damage?", while ignoring some of the above-mentioned challenges involving Ag-MAR implementation.

Preferably, Ag-MAR flooding is done during fallow or dormant periods, when crop damage is potentially minimal, so agricultural lands can serve as spreading basins for groundwater recharge. Root zone residence time (RZRT) is defined as the duration that the root-zone can remain saturated (or nearly saturated) during Ag-MAR without crop damage (O'Geen et al., 2015). RZRT is a crucial factor in Ag-MAR, as long periods of saturated conditions in the root-zone can damage crops due to oxygen deficiency (hypoxia) or complete depletion of oxygen

(anoxia), which ultimately may result in yield loss (Kozlowski, 1997). However, flood tolerance among crops varies considerably due to biotic and abiotic conditions (Schaffer et al., 1992), therefore only appropriate crops under specific conditions may be suitable for Ag-MAR application. For example, Dokoozlian et al. (1987) have found that grapevine during dormancy can be flooded for 32 days (with an average daily recharge of 8 cm) each year without yield loss. Dahlke et al. (2018a) recently investigated the effect of different Ag-MAR flooding schemes (max. average daily recharge of 25 cm) on established alfalfa fields. Results suggest a minimal effect on yield when dormant alfalfa fields on highly permeable soils are subject to winter flooding. On the other hand, some crops are sensitive even to short-period flooding. Kiwi vines for example, are highly sensitive to root anoxia with reported yield lost and vines death due to extreme rainfalls and/or shallow groundwater levels (Smith and Buwalda, 1994). In a study on peach trees, flood cycles of 12 h per day with 5 cm ponding, applied for two months, resulted in branches with lower diameter and length growth, as well as smaller, low-quality, fruits, compared to the control trees (Insausti and Gorjón, 2013). The above examples demonstrate the need for an RZRT planning tool that can estimate Ag-MAR flood duration with minimal crop damage.

Usually, when Ag-MAR water application starts, aeration of the root-zone will be quickly suppressed by a water-layer covering the soil surface, as it prevents oxygen transport to the root-zone in the gas phase. When water application ceases, re-aeration of the root-zone will depend on the soil's drainage rate that controls the formation of connected air pores between the root-zone and atmosphere (Fig. 1a). Hence, proper estimation of the planned flood duration during Ag-MAR requires prior knowledge of both crop characteristics and soil texture.

Only a few attempts for estimating RZRT during Ag-MAR were made, as Ag-MAR is a relatively new MAR technique. O'Geen et al. (2015) used a fuzzy logic approach to rate the RZRT during Ag-MAR, based on the harmonic mean of the saturated hydraulic conductivity (K_s) of all soil horizons, soil drainage class, and shrink-swell properties. Their RZRT rating was combined with other factors generating a Soil Agricultural Groundwater Banking Index (SAGBI, https://casoilresource.lawr.ucdavis.edu/sagbi/). Flores-Lopez et al. (2019) proposed a root-zone model that includes crop type, soil properties, and recharge suitability (based on SAGBI) to estimate water application, flooding duration, and the interval between water applications. Their model was integrated with a Groundwater Recharge Assessment Tool (GRAT; https://gratviewer.earthgenome.org/) to optimize Ag-MAR water
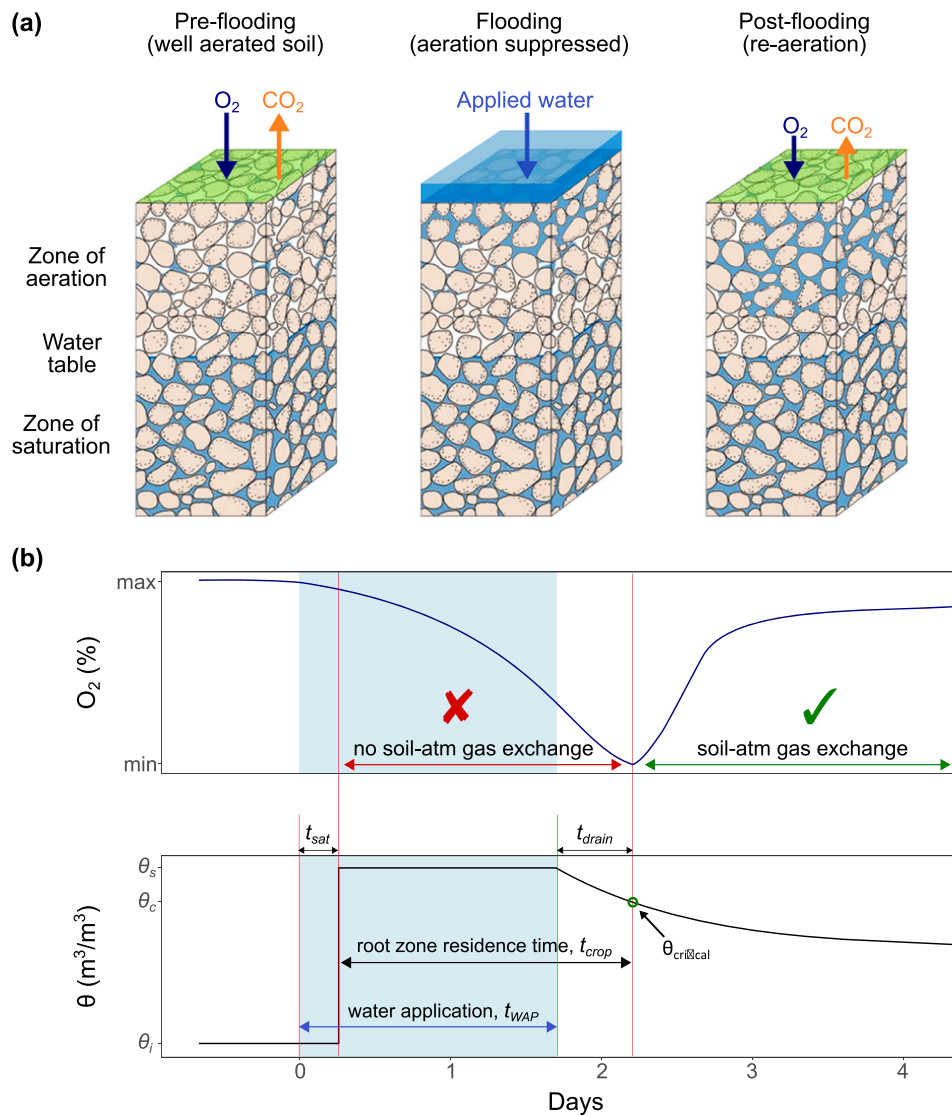

Fig. 1. (a) Conceptual model of the soil-atmosphere gas exchange during Ag-MAR under ponded conditions; and (b) the corresponding soil oxygen and water content profiles. The main parameters of the proposed model are also shown.
(modified from Ganot and Dahlke, 2021).

application.

Here, we propose a simple model to estimate the planned water application (flooding duration) during Ag-MAR based on the following parameters: (1) soil texture; (2) crop saturation tolerance; (3) effective root-zone depth; and (4) critical water content. The concept of critical water (or air) content was proposed by several authors (Freijer, 1994; Glinski and Stepniewski, 1985; Hamamoto et al., 2011; Hunt, 2005; Moldrup et al., 2005; Troeh et al., 1982) as it indicates a percolation threshold where the gas transport path is blocked by pore-water, which results in gas diffusivity and permeability of practically zero. Hence, when the water content is either below or above this threshold, gaseous oxygen transport into the soil is blocked or opened, respectively (Fig. 1b). As opposed to the previous Ag-MAR models mentioned above, our proposed model is physically based and includes explicitly the soil water content, that is used to infer the soil aeration status. Yet, thanks to its simplicity, this model can be integrated easily into various existing Ag-MAR assessment tools such as SAGBI (O'Geen et al., 2015) or GRAT (https://www.groundwaterrecharge.org/).

In the following, we first describe the theory of the model and the methods used to test the model performance. Next, we present the model predictions and compare them with observations and numerical simulations. Last, we present an example of how to calculate Ag-MAR water application duration and we discuss the applicability of the model and its limitations.

2. Methods

2.1. Model

We assume a one-dimensional (1D) ponded infiltration followed by drainage in a semi-infinite homogenous soil profile with deep groundwater. Hence, we neglect the presence of impermeable layers or shallow groundwater that may restrict deep percolation. Ponded infiltration is expected during Ag-MAR (Bachand et al., 2014; Dahlke et al., 2018a; Dokoozlian et al., 1987; Ganot and Dahlke, 2021) and the 1D assumption is justified by the relatively large horizontal dimensions of a flooded agricultural field (Philip, 1992) while the justification of the homogenous soil profile is site-specific. Water application duration (t_{wap}), with minimal crop loss, can be estimated based on crop tolerance to waterlogging (t_{crop}), time to saturate the soil (t_{sat}) up to the critical water content (θ_c) that blocks oxygen transport at the effective root-depth, and time to drain the soil (t_{drain}) back to θ_c to allow re-aeration of the effective root zone (Fig. 1b):

$$t_{wap} = t_{sat} + t_{crop} - t_{drain} \tag{1}$$

Note that it is assumed that the soil's O_2 storage can support soil respiration during the infiltration period (t_{sat}). This is supported by the analysis of Cook and Knight (2003) who showed that even under the extreme case of water saturation, dissolved oxygen in the water phase can support root respiration for a few hours and up to ~1.5 days, depending on temperature.

Each component of the proposed model, stated in the right-hand side of Eq. (1) is calculated separately. The period of ponded infiltration (t_{sat}) is calculated using the Green and Ampt (1911) model that includes the following simplified assumptions: constant ponding head, sharp wetting front with constant capillary pressure and constant (but different) water content on both sides of the wetting front. While these assumptions are seldom met in the field, the model has been widely used in hydrology due to its simplicity and accuracy (Selker and Assouline, 2017). Considering all of the above, the purpose of using the Green and Ampt approach here is mainly for estimating t_{sat}, i.e., the time to reach saturation at the effective root zone:

$$t_{sat} = \frac{(\theta_s - \theta_i)}{K_s} \left\{ z - (d - \psi_f) ln \left[\frac{z + d - \psi_f}{d - \psi_f} \right] \right\} \tag{2}$$

where θ_i and θ_s are the initial and saturated (or field saturated) volumetric water contents (L³ L⁻³), K_s is the saturated hydraulic conductivity (L T⁻¹), z [L] is the depth of the wetting front below the soil surface at time t_{sat}, here considered as the effective root depth, ψ_f (L) is the wetting front capillary head (negative value), and d [L] is the ponding depth. It is assumed that the soil profile portion that includes the effective root zone depth, attains field saturation during the Ag-MAR infiltration period. Hence, according to the sharp wetting front assumption, θ_i turns to θ_s at t_{sat}, so reaching the critical water content θ_c is not defined, and it is assumed that $\theta_c = \theta_s$ during the infiltration period. The parameter ψ_f was estimated by $\psi_f = \psi_a/2$ (Bouwer, 1966), where ψ_a is the air entry value; this estimation was found to be reasonably accurate for the purpose of predicting the wetting front depth (Ma et al., 2010). In this study we assumed $\psi_a = -1/\alpha$ where α is a fitting parameter in the soil water retention curve (SWRC) of van Genuchten (1980), resulting in $\psi_f = -1/(2\alpha)$. For simplicity (and in some cases lack of data), the ponding depth was taken as $d = 0$; i.e., it is assumed that water supply during Ag-MAR events will be according to the infiltration capacity of the specific Ag-MAR site (practically, initial water supply will be some finite rate higher than K_s, which eventually will be reduced to K_s). Note that Eq. (1) is not applicable when the water supply rate is lower than K_s; however, such low rates are inefficient when it is required to spread large volumes of water with flood irrigation infrastructure over large fields, and therefore are less expected during Ag-MAR operation.

A literature review was used to collect data of t_{crop} which is based on controlled studies as well as on growers and specialists' experience.

The drainage period t_{drain} is calculated based on the solution of Sisson et al. (1980) to the 1D Richards equation assuming gravity is the dominant driving force (unit gradient) during the drainage phase:

$$\frac{\partial \theta}{\partial t} = -\frac{\partial K}{\partial z} = -\frac{dK(\theta)}{d\theta}\frac{\partial \theta}{\partial z} \tag{3}$$

where z is the depth (positive downward; soil surface at $z = 0$), and the conditions for the drainage period include a zero flux at the soil surface and an initially saturated soil profile. Note that the assumption of a unit gradient during drainage is acceptable for uniform soil profiles (Ahuja et al., 1988; Sisson and Van Genuchten, 1991), which was assumed in this model. Based on the approach of Lax (1972) the solution for the characteristic curves of Eq. (3) is given by (Sisson et al., 1980):

$$K'(\theta) = \frac{dK}{d\theta} = \frac{z}{t_{drain}} \tag{4}$$

According to this solution, the drainage "front" (i.e., the boundary between the saturated profile and the desorption zone above it) advances at a constant rate of $\left.\frac{dK}{d\theta}\right|_{\theta_s}$ (see Fig. 2 in Sisson et al., 1980). This solution is less accurate in shallow depths but was found accurate when compared with a numerical solution, with a maximum water content deviation of 0.01 cm³/cm³ for $z > 25$ cm (Sisson et al., 1980). According to Eq. (4), knowing the hydraulic conductivity function $K(\theta)$ allows estimation of t_{drain} for a given effective root depth, z. For the soil hydraulic functions of van Genuchten (1980) and Mualem (1976), Eq. (4) will take the following form (Sisson and Van Genuchten, 1991):

$$K'(\theta) = K_s \frac{(1 - A^m)(1 - A^m + 4S^{1/m}A^{m-1})}{2(\theta_s - \theta_r)\sqrt{S}} \tag{5}$$

where $S = (\theta-\theta_r)/(\theta_s-\theta_r)$ is the effective saturation and $A = 1-S^{1/m}$ where $m = 1-1/n$, and n is a shape parameter in the soil water retention curve (SWRC) of van Genuchten (1980). Eq. (5) can be solved for the drainage time until a critical water content is reached where re-aeration of the root zone is achieved:

$$t_{drain} = \frac{z}{K_s} \frac{2(\theta_s - \theta_r)\sqrt{S_c}}{(1 - A_c^m)(1 - A_c^m + 4S_c^{1/m}A_c^{m-1})} \tag{6}$$

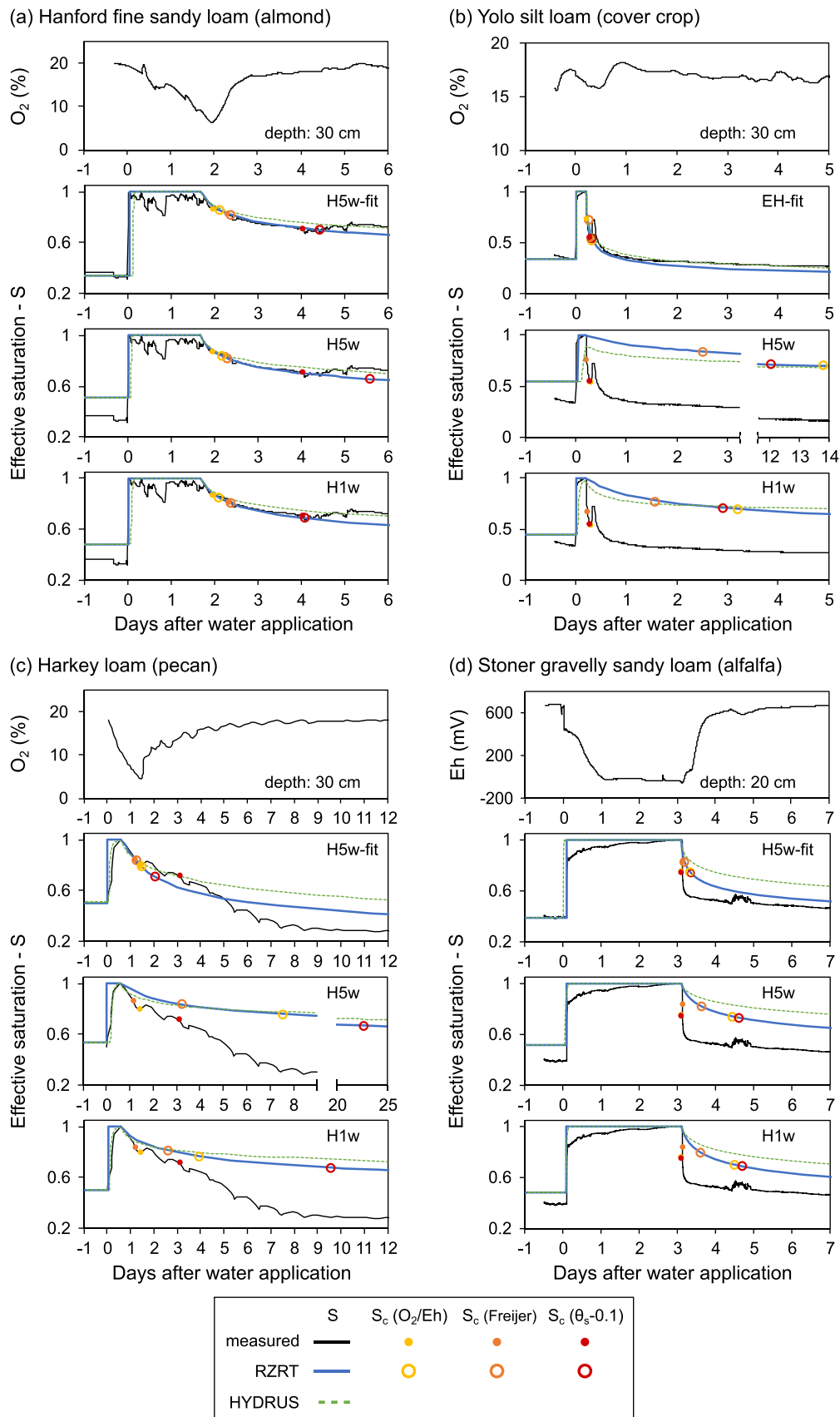**Fig. 2.** Predicted and observed effective saturation (S). (a) Hanford fine sandy loam; (b) Yolo silt loam; (c) Harkey loam; (d) Stoner gravelly sandy loam. H5w-fit/EH-fit, H5w, and Hw1 represent different hydraulic parameter sets (see details in Table 1). Soil oxygen or redox potential data are presented in the top plot of each soil. Data from: Ganot and Dahlke (2021) (a, b); Kallestad et al. (2008a) (c); and Dahlke et al., 2018a (d).

where $S_c = (\theta_c-\theta_r)/(\theta_s-\theta_r)$ is the critical effective saturation corresponding to the critical water content (θ_c) at depth z, and $A_c = 1-S_c^{1/m}$.

2.2. Model testing

Field data of four soils from Ag-MAR and flood irrigation studies (Dahlke et al., 2018a; Ganot and Dahlke, 2021; Kallestad et al., 2008a) were used to test the model. Data included volumetric water content and soil oxygen (or redox potential) that were used to obtain θ_c for each soil. For more details on the adequacy of these measurements to quantify the soil aeration status under flooded conditions see Mukhtar et al. (1996), Kallestad et al. (2008b) and Ganot and Dahlke (2021). We defined the measured θ_c as the soil water content value after which soil oxygen recovery begins (i.e., when soil respiration $\approx$ oxygen supply; see the minimum point on the O_2 curve in Fig. 1b). The hydraulic parameters of the model (θ_r, θ_s, α, n, K_s) were calculated using the pedo-transfer functions (PTF) code Rosetta3 (Zhang and Schaap, 2017), based on soil properties of the National Cooperative Soil Survey (NCSS, 2020) obtained through the SoilWeb app (O'Geen et al., 2017). For each soil, we tested the model with three different sets of hydraulic parameters. Following the nomenclature of Rosetta3, the three modeling scenarios are (1) H5w-fit: PTF is based on soil texture, bulk density, and water content at 330 and 15,000 cm suction; θ_i, θ_s and in some cases n or K_s are calibrated to observed data; (2) H5w: PTF is same as H5w-fit, but no calibration was performed; and (3) H1w: PTF is based on average hydraulic parameters of the USDA textural classes. For the Yolo silt loam soil, we used hydraulic parameters from Eching and Hopmans (1993), instead of H5w-fit (labeled as EH-fit) because of its poor performance. For the hydraulic parameter sets (2) and (3) θ_i was assumed to equal field capacity (θ_{FC}), calculated as suggested by Assouline and Or (2014) using the SWRC hydraulic parameters:

$$\theta_i = \theta_{FC} = \theta_r + (\theta_s - \theta_r)\left[1 + \left\{\left(\frac{n-1}{n}\right)^{(1-2n)}\right\}\right]^{\left(\frac{1-n}{n}\right)} \tag{7}$$

The model goal is to estimate flooding duration and therefore we tested whether the model can accurately predict the time when the critical water content (θ_c) is reached, which is the time when re-aeration of the soil profile started. In addition to the measured θ_c, we also tested θ_c of Freijer (1994) which showed that the van Genuchten (1980) approximated air-entry value ($-1/\alpha$) is a good estimate for evaluating θ_c:

$$\theta_c = \theta_r + \frac{(\theta_s - \theta_r)}{2^m} \tag{8}$$

Eq. (8) is obtained by setting the matric head in van Genuchten (1980) SWRC equal to $-1/\alpha$; hence, it allows estimating θ_c based solely on the SWRC parameters. Another common θ_c that was tested is $\theta_c = \theta_s - 0.1$ (i.e., assuming a constant critical air content of 0.1 for soil aeration), which was suggested by several authors (Grable and Siemer, 1968; Silva et al., 1994; Troeh et al., 1982; Wesseling and Van Wijk, 1957). The percolation threshold of Hunt (2004) can also be used to estimate θ_c, but it was not tested here because both Freijer (1994) and measured θ_c values were usually within the range suggested by Hunt (2004). Note that in order to compare models of the same soil type but with different θ_s, the θ_c was adjusted according to $\theta_{c, new} = \theta_{s, new} - (\theta_s - \theta_c)$; where ($\theta_s - \theta_c$) is the critical air content. In other words, we assumed that for each soil texture the critical air content (i.e., the percolation threshold, or the inactive air-filled pore-space) remains constant (Moldrup et al., 2005). This excludes the θ_c of Freijer (1994) which was determined by the SWRC parameter m ($= 1-1/n$). The hydraulic parameters used for testing the model are summarized in Table 1.

The model was further tested using simulations of the infiltration and drainage processes. The numerical flow and transport model HYDRUS-1D (Šimůnek et al., 2009) was used to simulate Ag-MAR flooding in the soils listed in Table 1 (i.e., a total of 12 simulations: 4 soils, each with 3 different sets of hydraulic parameters). Boundary conditions at the soil surface assumed a constant head ($d = 0$) during infiltration and zero flux during drainage; at the bottom of the domain, we assumed a free drainage boundary (unit gradient). Evaporation and root water uptake were neglected. A homogenous soil profile of 5 m with (vertical) discretization of 0.5 cm was used for all simulations. The soil profile depth was selected to prevent the wetting front from reaching the lower boundary, but for two cases where K_s was very high (and/or flooding time was long), deeper soil profiles were needed: 7.5 m for the Yolo silt loam (H5w-fit), and 20 m for the Stoner Gravelly sandy loam (H5w-fit). The default iteration criteria and time discretization of HYDRUS-1D were used, except for the smaller initial time step (10^{-4} day) to overcome convergence issues during infiltration.

Since low K_s layers such as hardpans are quite common features in agricultural soils, we also tested the insertion of hardpan layer in the proposed RZRT model. We recognize two cases: (1) when the effective root depth (z) is deeper than the hardpan layer; and (2) when z is shallower than the hardpan layer. For case 1 an effective K_s is calculated using z as the total depth; for case 2 (deeper hardpan) we tested whether the hardpan layer impacts the drainage in the root zone by calculating the time it takes for the wetting front to reach the hardpan layer ($t_{hardpan}$) using the Green and Ampt model with setting z in Eq. (2) as the hardpan layer depth. When $t_{hardpan} > t_{sat} + t_{crop}$ the effective root depth is not impacted by the deeper hardpan layer and the original K_s is used

Table 1
Hydraulic parameters used in the model.

Soil	Crop	Hydraulic parameters	z (cm)	ψ_f (cm)	θ_i	θ_c measured	θ_c Freijer (1994)	θ_c θ_s-0.1	θ_r	θ_s	α (1/cm)	n	K_s (cm/day)
Hanford fine sandy loam	Almond	H5w-fit	30	21.05	0.155[a]	0.330	0.316	0.276	0.042	0.376[a]	0.0238	1.400	42.6
		H5w	30	21.05	0.191	0.288	0.282	0.234	0.042	0.334	0.0238	1.400	42.6
		H1w	30	30.48	0.215	0.335	0.318	0.281	0.061	0.381	0.0164	1.457	37.4
Yolo silt loam	Cover crop	EH-fit[b]	30	13.89	0.302[a]	0.343	0.386	0.347	0.228	0.447[a]	0.0360	1.905	435
		H5w	30	81.12	0.287	0.340	0.389	0.301	0.099	0.444	0.0062	1.340	14.6
		H1w	30	145.76	0.236	0.323	0.352	0.327	0.083	0.427	0.0034	1.552	18.5
Harkey loam	Pecan	H5w-fit	30	58.10	0.227[a]	0.324	0.341	0.297	0.055	0.397[a]	0.0086	2.142[a]	11.1
		H5w	30	58.10	0.217	0.283	0.306	0.255	0.055	0.355	0.0086	1.347	11.1
		H1w	30	78.64	0.246	0.330	0.344	0.302	0.090	0.402	0.0064	1.421	13.3
Stoner gravelly sandy loam	Alfalfa	H5w-fit	20	63.21	0.212[a]	0.351	0.379	0.347	0.062	0.447[a]	0.0079	1.387	242[c]
		H5w	20	63.21	0.256	0.340	0.370	0.336	0.062	0.436	0.0079	1.387	43.7
		H1w	20	30.48	0.215	0.285	0.318	0.281	0.061	0.381	0.0164	1.457	37.4

SWRC parameters were calculated with Rosetta3 (Zhang and Schaap, 2017) based on soil properties from the NCSS database (NCSS, 2020, unless otherwise stated).
[a] fitted parameters;
[b] parameters from Eching and Hopmans (1993);
[c] parameter from SSURGO database.

for calculations; when $t_{hardpan} \leq t_{sat} + t_{crop}$ the effective root depth is impacted by the hardpan layer and an effective K_s is calculated using the bottom depth of the hardpan layer as the total depth. In both cases, the other SWRC parameters are left unchanged (i.e., equal to the SWRC parameters of the original layer). For each case, we tested the RZRT model with the arithmetic and harmonic mean of K_s, and compared the results to the HYDRUS simulation of the Hanford fine sandy loam (H5w-fit). Overall settings of the simulation domain were similar to the conditions noted above (top: constant ponding head, $d = 0$; bottom: free drainage) with the addition of a hardpan layer. The effective root depth was 30 cm and the hardpan layer thickness was taken as 20 cm with a hydraulic conductivity of $0.1K_s$.

2.3. Drainage curves

It is clear from Eq. (1) that minimal water application for Ag-MAR ($t_{wap} > 0$) is attained only when the condition $t_{drain} < t_{sat} + t_{crop}$ is met. As a first approximation of Ag-MAR adequacy for different soil textures, we tested the condition $t_{drain} < t_{crop}$ by calculating drainage curves (t_{drain}) for each USDA soil texture class using Eq. (6). Calculating the drainage curves using Eq. (6) requires the SWRC hydraulic parameters (θ_r, θ_s, n, K_s), the critical water content θ_c, and the effective root zone depth z. The hydraulic parameters were estimated based on soil texture data using PTF of the USDA soil texture classes (H1w in Rosetta3, Zhang and Schaap, 2017), while θ_c was taken as $\theta_c = \theta_s - 0.1$ (a conservative assumption), and three representative values of z were used (25, 50 and 100 cm).

3. Results and discussion

3.1. Crop parameters

3.1.1. Effective root depth (z)

Root depth varies among crops and fields as it depends on crop type and age, irrigation method, soil texture, soil layering and restrictive layers or shallow groundwater (Gilman, 1990). Maximum root depths

for several crops are given in Table 2 based on the FAO guidelines (Allen et al., 1998). However, using these maximum root depths values in the model proposed in this work will give a relatively conservative (i.e., short) water application duration for Ag-MAR. Practically, in most orchards, the effective root depth (where root activity is highest) is usually located in the upper 0.5 m of the soil profile (Atkinson, 1983; Gilman, 1990; Lehmann, 2003; Nethsinghe and Broeshart, 1975). Examples of the effective root depth of several crops obtained from the literature are also provided in Table 2. Alternatively, the root depth and distribution can be estimated in-situ based on invasive (Oliveira et al., 2000; van Noordwijk et al., 2000) and non-invasive techniques (Amato et al., 2008; Hruska et al., 1999).

3.1.2. Crop tolerance to flooding

Plant tolerance to flooding or the duration of flooding with minimal crop damage (t_{crop}) is a very challenging parameter to estimate. A tremendous diversity of tolerance exists, which depends on several factors: (1) soil texture and chemistry; (2) degree and duration of hypoxia/anoxia; (3) soil microbe and pathogen status; (4) vapor pressure deficit (VPD), and root-zone and air temperatures; (5) plant species, age, stage and season of the year; and (6) plant adaption as a result of prior climate and soil conditions (Schaffer et al., 1992). An estimate of crop tolerance to flooding of common perennial crops is provided in Table 3, which is an extended version of a previous survey (Table 1 in O'Geen et al., 2015). Annual crops were not included in Table 3 because it was assumed that these fields usually would be fallow during winter and spring when excess surface water is available for Ag-MAR (Kocis and Dahlke, 2017; O'Geen et al., 2015; USDA, 2007, 2010). Waterlogging tolerance in most fruit trees is mainly determined by the rootstock and not by the scion (Schaffer et al., 1992), where tolerance is higher during dormancy, but more prone to damage during bud break and growth (O'Geen et al., 2015). The plant tolerance scales in Table 3 have different definitions, as some authors use plant survival as the tolerance criterion, while others consider economical damage (such as growth or yield reduction) as the tolerance criterion; these differences are indicated in Table 3. We note that the data provided in Table 3 should be

Table 2
Root depth of selected crops.

Crop	Maximum root depth (m)[a]	Effective root depth, z (m)[b]	Roots (% of total)	plant age (years)	Soil texture (USDA)	Irrigation method	Source
Alfalfa	1–2	1.36	95	n/a[c]	n/a[c]	n/a[c]	Fan et al. (2016)
Almond	1–2	0.3[d]	n/a	6	gravely sandy loam	micro-sprinklers	Koumanov et al. (2006)
Apple	1–2	0.8	100	10	clay loam	drip	Sokalska et al. (2009)
Apricot	1–2	0.5	91	18	loam	drip	Ruiz-Sánchez et al. (2005)
Avocado	0.5–1	0.5	72	8	loam	drip	Michelakis et al. (1993)
Blueberry	0.6–1.2	0.5/0.7	100	8/38	sandy loam	sprinklers	Paltineanu et al. (2018)
Cherry	1–2	0.5	n/a	8	sandy loam	drip	Paltineanu et al. (2017a)
Citrus	0.8–1.5	0.4[d]	n/a	12	clay	drip	Panigrahi and Srivastava (2016)
Cranberry	0.6–1.2	0.3	n/a[c]	n/a[c]	n/a[c]	sub-irrigation, sprinklers	Sandler et al. (2004)
Grape	1–2	1	100	4	sandy loam	micro-sprinklers, drip	Bassoi et al. (2003)
Kiwi	0.7–1.3	0.8	100	7	fine sandy loam, fine sand, gravelly coarse sand	mini-sprinklers	Green and Clothier (1995)
Papaya	n/a	0.55	100	n/a[c]	n/a[c]	micro-sprinklers, drip	Carr (2014)
Peach	1–2	0.3	90	5	loamy sand	drip	Lopes et al. (2014)
Pear	1–2	0.8	100	8	silt loam	drip	Wang et al. (2020)
Plum	1–2	0.9	100	6	sandy loam	drip	Paltineanu et al. (2017b)
Quince	1–2	0.4[e]	80	6	clay loam	rainfed	Machado et al. (2018)
Walnut	1.7–2.4	0.8	100	2	loamy sand	flood	Duan et al. (2019)

[a] FAO guidelines (Allen et al., 1998);
[b] obtained by root measurements, unless otherwise stated;
[c] see details in source reference;
[d] based on soil water content analysis;
[e] rootstock for pear.

Table 3
Crop tolerance to flooding.

crop	Rootstock	Dormancy saturation tolerance	Growth saturation tolerance	Source
Alfalfa[a]		n/a	2–3	Barta (1988); Thompson and Fick (1981)
Almond[a]	Peach; peach x almond hybrid	1	1	O'Geen et al. (2015)
Almond[a]	Plum; peach x plum hybrid	2–3	1	O'Geen et al. (2015)
Apple[a]		4	2	Lasko (1994)
Apricot		1	1	(Schaffer et al., 1992)
Avocado		0	0	(Schaffer et al., 1992); O'Geen et al. (2015)
Blueberry		4	2–4	Davies and Darnell (1994)
Cherry[a]		1	0	Beckman et al. (1986); O'Geen et al. (2015)
Citrus		0	0	O'Geen et al. (2015)
Citrus	rough lemon	2–3	2–3	(Schaffer et al., 1992); Bhusal et al. (2002)
Citrus	trifoliate orange	2–3	2–3	(Schaffer et al., 1992); Bhusal et al. (2002)
Cranberry[a]		1	1	Davies and Darnell (1994)
Grape[a]		4	2	Dokoozlian et al. (1987); O'Geen et al. (2015)
Kiwi		0	0	(Schaffer et al., 1992)
Papaya		0	0	(Schaffer et al., 1992)
Peach		1	n/a	Chaplin et al. (1974)
Pear[a]	P. betulaefolia	4	4	O'Geen et al. (2015)
Pear[a]	P. communis	4	3	O'Geen et al. (2015)
Pear[a]	Cydonia oblonga	3–4	2–3	O'Geen et al. (2015)
Pecan		4	2–3	Andersen (1994); Kallestad et al. (2007)
Plum/Prune[a]	Peach	1	1	O'Geen et al. (2015)
Plum/Prune[a]	Plum; peach x plum hybrid	2–3	1	O'Geen et al. (2015)
Quince		4	4	Mitchell et al. (1994)
Walnut		2–4	1	Andersen (1994); O'Geen et al. (2015)

Tolerance scales indicate plant survival unless otherwise stated.
The following scores were used to estimate vulnerability (O'Geen et al., 2015): 0 - No tolerance for standing water; 1 - tolerant of standing water up to 48 h; 2 - tolerant of standing water up to 1 week; 3 - tolerant of standing water up to 2 weeks; 4 - tolerant of standing water > 2 weeks. [a]Tolerance indicates economical damage. Data provided in Table 3 is mainly based on expert opinion and to a lesser extent on controlled experiments.

used with caution because most of it is based on expert opinion or experiments with seedlings, while very few waterlogged experiments were conducted with bearing fruit trees.

3.2. Model testing

The predicted and observed effective saturation (S) results are presented in Fig. 2, along with the corresponding soil oxygen or redox potential that were used to obtain the measured θ_c (shown as S_c in Fig. 2, where $S_c = [\theta_c-\theta_r]/[\theta_s-\theta_r]$).
The three S_c (measured, Freijer, 1994 and θ_s-0.1) are marked by open

and filled circles for the predicted and observed effective saturation, respectively. Graphically, when the open and filled circles (S_c) of the same color are closer, the RZRT model predictions are better. As already motioned, the RZRT model goal is to estimate Ag-MAR water application duration (t_{wap}), and therefore we tested the time difference between predicted and observed S_c. As expected, the error ($e = t_{wap, \, predicted} - t_{wap, \, observed}$) and mean absolute error ($MAE = n^{-1}\sum_{i=1}^{n}|e_i|$) are lowest for the fitted RZRT models (H5w-fit and EH-fit) followed by Hw1 and H5w (Table 4). In all cases, the error is close to zero or positive, i.e., the predicted t_{wap} is similar or overestimates the observed t_{wap} (excluding one case of underestimation by 1 day). This means that for highly

Table 4
(a) Water application duration error ($t_{wap, \, predict} - t_{wap, \, observed}$) for the tested soils.

Soil	Hydraulic parameters	θ_c measured Error (days)	θ_c Freijer (1994) Error (days)	$\theta_c = \theta_s$-0.1 Error (days)
Hanford fine sandy loam	H5w-fit	0.12	0.05	0.35
	H5w	0.17	0.04	1.52
	H1w	0.10	0.05	0.01
Yolo silt loam	EH-fit	0.01	0.01	0.02
	H5w	13.48	2.26	11.75
	H1w	2.88	1.31	2.61
Harkey loam	H5w-fit	0.00	0.00	-1.08
	H5w	6.09	2.04	19.5
	H1w	2.47	1.35	6.41
Stoner gravelly sandy loam	H5w-fit	0.20	0.06	0.23
	H5w	1.31	0.48	1.48
	H1w	1.37	0.43	1.56

(b) Mean absolute error (MAE) of the different RZRT models and θ_c.

MAE (days)	θ_c measured	θ_c Freijer (1994)	$\theta_c = \theta_s$-0.1	Avg.
H5w-fit	0.08	0.03	0.42	0.18
H5w	5.26	1.20	8.56	5.01
H1w	1.70	0.79	2.65	1.71
Avg.	2.35	0.67	3.88	

sensitive crops the model should be used with caution. When testing the *MAE* of the RZRT models by its θ_c, the RZRT models with θ_c of Freijer (1994) has the lowest *MAE*, followed by the measured θ_c and θ_s-0.1 (Table 4b). θ_c of Freijer (1994) outperforms the measured θ_c probably because its estimated θ_c obtained at higher water contents where the deviations of measured water contents and the RZRT model are minimal.

The fit between the predicted and observed effective saturation ranges from poor (e.g., H5w in Fig. 2b) to excellent (e.g., H5w-fit in Fig. 2a), and generally the fit is better for the RZRT models that underwent calibration (H5w-fit and EH-fit) followed by Hw1 and H5w.

Obviously, a better fit of the predicted and observed water contents will lead to a more accurate estimation of t_{wap}. Therefore, when possible, it is recommended to use the proposed RZRT model with site-specific hydraulic parameters. This is demonstrated in the Yolo silt loam soil, where a reasonable fit was not feasible without the use of site-specific hydraulic parameters (EH-fit, Fig. 2b). Note that site-specific parameters can vary considerably for the parameters obtained from the NCSS database. This is especially notable for the *Ks* values which can vary by more than one order of magnitude (e.g., see Yolo and Stoner soils in Table 1). The reason for this discrepancy is attributed to the low spatial representation of each soil series in the NCSS database, which is based on few soil pedons that are not always a good representation of the soil series where the field data was collected. In some cases, even when the overall effective saturation fit is poor, it is possible to estimate t_{wap} accurately given that the fit is good at the range of S_c. This is demonstrated in the Harkey loam for the H5w-fit (Fig. 2c). Note that for all soils H1w performs better than H5w, supposedly not as expected, because Rosetta3 is a hierarchical PTF where the highest hierarchy (H5w) should perform better than lower hierarchies (H1w-H4w, Zhang and Schaap, 2017). As noted above, this is because each of the H5w parameters in this study was based on only one soil pedon sample from a specific location (as provided by the NCSS database), which in this study was less representative compared to the Hw1 parameters that are based on averaging by soil texture a large number of soil samples.

The fit of the effective saturation between the proposed RZRT model and the numerical model HYDRUS-1D ranges from good to excellent (by visual inspection; Fig. 2), and in all cases, HYDRUS fits better to the RZRT model than to the observed data. This indicates that the deviations between the RZRT model predictions and the observed water content data are probably due to soil layering, soil heterogeneity, and preferential flow, which cannot be captured by simplified homogenous one-dimensional flow models. Another explanation for the observed and modeled water content deviations could be an inappropriate setting of the models' boundary conditions. This mainly refers to the assumption of free drainage at the bottom boundary because the top boundary was controlled during the experiments.

3.3. Total Ag-MAR water application

The proposed model goal is to estimate Ag-MAR duration with minimal crop damage, but we also tested whether it can be used to estimate total water application. We assumed the total water application equals the cumulative infiltration (I) which can be described by an explicit solution of the Green and Ampt model (Selker and Assouline, 2017):

$$I = tK_s - \psi_f(\theta_s - \theta_i)ln\left[1 + A\frac{tK_s}{-\psi_f(\theta_s - \theta_i)} + \sqrt{\frac{2tK_s}{-\psi_f(\theta_s - \theta_i)}}\right] \quad (9)$$

where $t = t_{wap}$ (calculated with Eq. (1)) and A is an empirical factor in the range of 1/3–1, here taken as 2/3 as proposed by Selker and Assouline (2017). We compared the total water application predicted by the RZRT model (Eq. (9)) and HYDRUS with the observed data (Table 5). Generally, the RZRT model with fitted parameters overestimates the prediction of HYDRUS and the observed total water application, while H5w and H1w shows highly variable estimations. Hence, the large variability in the model predictions implies it can be used only as a first approximation for estimating Ag-MAR total water application amounts.

3.4. Hardpan layer

The performance of the RZRT model with a hardpan layer above or below the effective root zone was compared to HYDURS simulations with similar settings (Fig. 3). According to our limited test, the RZRT model with the harmonic mean K_s is preferred during the infiltration period. During the drainage period the arithmetic or the harmonic mean K_s are preferred when the hardpan layer is above or below the effective root zone, respectively. As expected, when the hardpan layer is far below the effective root zone (i.e., when $t_{hardpan} > t_{sat} + t_{crop}$) there is no impact on the effective root zone by the hardpan. The total water applied calculated with Eq. (9) and the harmonic mean K_s is almost identical to the HYDRUS results (Fig. 3). This demonstrates the impact of a hardpan on deep percolation, as the total water amounts applied were reduced by more than half when the hardpan layer was close to the root zone. Based on the preferred effective K_s, the highest θ_c deviation between the RZRT model and HYDRUS is one day. While this is a reasonable error for the hardpan characteristics tested here, it is based on one limited example and cannot be regarded as representative. Using effective soil hydraulic parameters to represent highly-contrast layered soil as a uniform soil profile is a complex problem (Nasta and Romano, 2016) which was beyond the scope of our simplified analysis. Hence, the hardpan analysis implemented in the RZRT learning tool (see next section) can be used as a first approximation only. Obviously, in fields with a massive hardpan layer, deep percolation is limited, and implementation of Ag-MAR project is not recommended.

3.5. Example: calculating Ag-MAR flood duration for grapevine in sandy loam soil using the RZRT learning tool

To demonstrate the applicability of the model, we applied the RZRT model to the Hanford fine sandy loam (H5w-fit; see Table 1 for hydraulic parameters), assuming an effective root depth for grapevine of 1 m (Table 2), and a saturation tolerance of $t_{crop} = 7$ days (Table 3). We calculate $t_{sat} = 0.33$ days (Eq. (2)) and $t_{drain} = 1.34$ days (Eq. (6); using the measured θ_c from Table 1). Hence, water application duration for Ag-MAR based on Eq. (1) is: $t_{wap} = t_{sat} + t_{crop} - t_{drain} = 0.33 + 7-1.34 \approx 6$ days. A first approximation of the total water applied for 6 days is $I = 2.7$ m (Eq. (9)). The above example was quickly calculated using the RZRT learning tool, found in the Supplemental
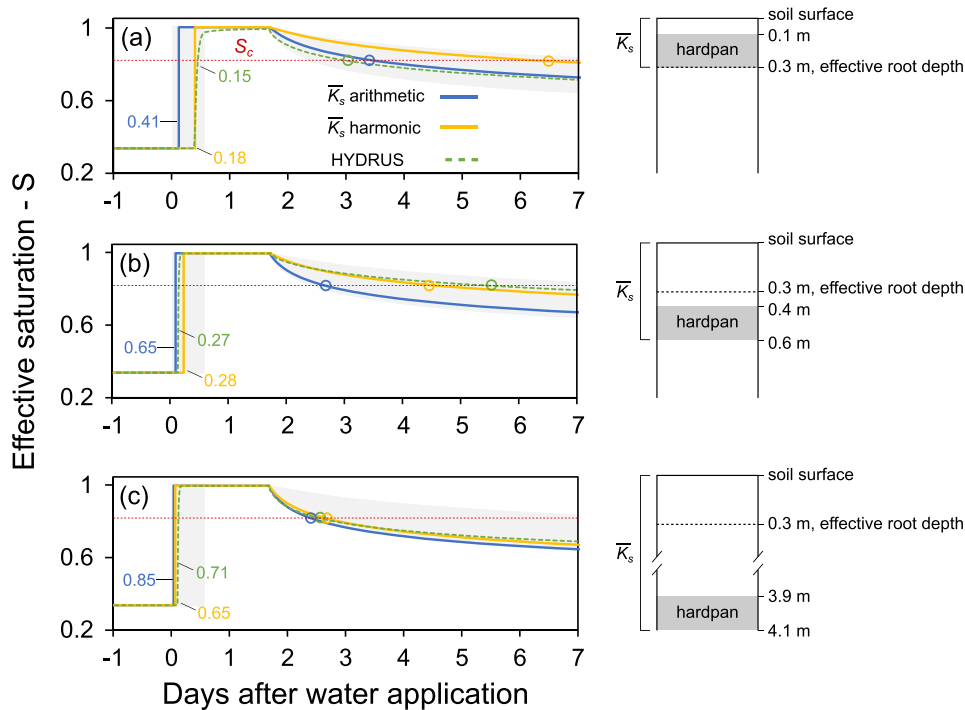
Table 5
Total water applied (WAP) estimated by the different models and the relative error (RE) compared to the observed WAP.

Soil	Hydraulic parameters	RZRT model		HYDRUS		Observed
		WAP (m)	RE (%)	WAP (m)	RE (%)	WAP (m)
Hanford fine sandy loam	H5w-fit	0.85	12	0.71	-7	0.76
	H5w	0.81	7	0.70	-8	
	H1w	0.77	1	0.62	-18	
Yolo silt loam	EH-fit	0.94	130	0.88	115	0.41[a]
	H5w	0.11	-74	0.05	-88	
	H1w	0.17	-59	0.11	-73	
Harkey loam	H5w-fit	0.16	20	0.21	56	0.13
	H5w	0.15	12	0.08	-41	
	H1w	0.20	46	0.11	-18	
Stoner gravelly sandy loam	H5w-fit	8.07	314	7.19	269	1.95
	H5w	1.66	-15	1.33	-32	
	H1w	1.32	-32	1.15	-41	

RE = (WAP$_{predicted}$ / WAP$_{observed}$) − 1;
[a] upper bound estimation

Fig. 3. Effective saturation (S) of the RZRT model with effective K_s, compared to HYDRUS simulations with hardpan layer. Schematic soil profiles on right shows hardpan location for each case. (a) effective root zone below hardpan; (b) effective root zone above (or within) hardpan; and (c) hardpan deep below the effective root zone. Open circles are the critical effective saturation (S_c) of Freijer (1994) and numbers represent total applied water (m). Shaded background is bounded by maximum K_s (soil) and minimum K_s (hardpan).

Material. The RZRT learning tool is an MS Excel workbook that includes several worksheets with the equations and tables listed in this paper. The main worksheet is used for all data inputs and outputs. For calculating water application duration, the user can select pre-defined (tabulated) parameters in the worksheet or enter site-specific values. To date, our database of measured θ_c is limited due to the finite number of experimental sites we have collected data from, but the user can also select between θ_c of Freijer (1994), $\theta_c = \theta_s - 0.1$, or some user-defined θ_c.

3.6. Drainage curves

The drainage curves for all USDA soil texture classes provide an initial estimation of soil suitability for Ag-MAR (Fig. 4). The crops almond, walnut, alfalfa, and grape in Fig. 4 with flooding tolerance of 2, 7, 14, and 21 days, respectively, represent the four tolerance classes in Table 3. Since crops have different flooding tolerances, soil drainage largely controls the effective flooding duration. The slow drainage rate combined with the low flooding tolerance that some perennial crops have, make clayey soils, as expected, unsuitable for Ag-MAR. The clay loam soil with shallow-rooted high-tolerance crops, might be suitable for Ag-MAR in terms of drainage duration, however, its ability to transfer large quantities of water is hindered by its relatively low hydraulic conductivity ($K_s = 7$ cm day^{-1}) questioning its Ag-MAR suitability. The silty clay loam is an exception of the clayey soils, as it can be used for Ag-MAR with moderate- and high-tolerance crops. The reason for this exception is the low sand content combined with the silt and clay proportions, which results in a higher critical water content (as θ_c) as aggregated soils have higher θ_c (or lower critical air content) compared to structureless sandy soils (Ben-Noah and Friedman, 2018; Cook et al., 2013). For the same reason, loam soil with lower θ_c can be used only for Ag-MAR if shallow-rooted moderate- and high-tolerance crops are considered. According to the drainage curves, silt loam and sandy loam soils are suitable for all crops, excluding minimal-tolerance crops, while sand, silt and loamy sand soils are suitable for all crops that have minimal flooding tolerance.

3.7. Model limitations

The main model limitations are related to the assumption of 1D flow in a homogenous soil profile. For most Ag-MAR sites with contrasting soil layering along the root zone, the model prediction will be less accurate, and a procedure of parameter averaging may be necessary to improve the model performance. Similar model limitations that are related to the homogenous soil profile assumption, are expected at sites with substantial soil heterogeneity, as our results show for the Stoner gravelly sandy loam (Fig. 2d). A reasonable estimation of the hydraulic parameters is another limitation that should be considered. For example, according to the soils tested in this work, when using fitted (H5w-fit/EH-fit) and average unfitted (H1w) hydraulic parameters, t_{wap} is overestimated by 0.2 and 1.7 days, on average, respectively (Table 4b).

The model assumption of rigid porous media with constant hydraulic properties poses another difficulty, especially under Ag-MAR conditions where the soil can be waterlogged for relatively long periods (compared to conventional agricultural practices). Changes in soil structure and hydraulic properties during prolonged flooding were reported in paddy soils due to clay swelling (e.g., Zhang et al., 2013); however, shrink-swell dynamics are more prominent in clayey soils (Horn et al., 2014), which are potentially less suitable for Ag-MAR.

The use of hydraulic parameters from a soil database (such as the NCSS used in this study) can lead to moderate or poor predictions compared to soil-specific hydraulic parameters. The shape parameter m and the scale parameters θ_r, θ_s and K_s control the drainage curves (Eq. (6)) and therefore are the most important parameters in the RZRT model. For improved accuracy, these parameters should be evaluated in-situ at the designated Ag-MAR site. θ_r and θ_s can be estimated by the gravimetric method (Topp and Ferré, 2002) and K_s of the upper soil by various field infiltration tests (Angulo-Jaramillo et al., 2019; Nimmo et al., 2009; Reynolds et al., 2002). Estimating m can be attained by fitting of the SWRC (Dane and Hopmans, 2002) or the particle size distribution (Lassabatère et al., 2006); however, these methods are time-consuming, so it is recommended to obtain m from a soil database, the literature, or to use a pre-defined m based on soil texture.

Lastly, and probably most importantly, the parameter estimation of θ_c can change markedly depending on the method it was first evaluated
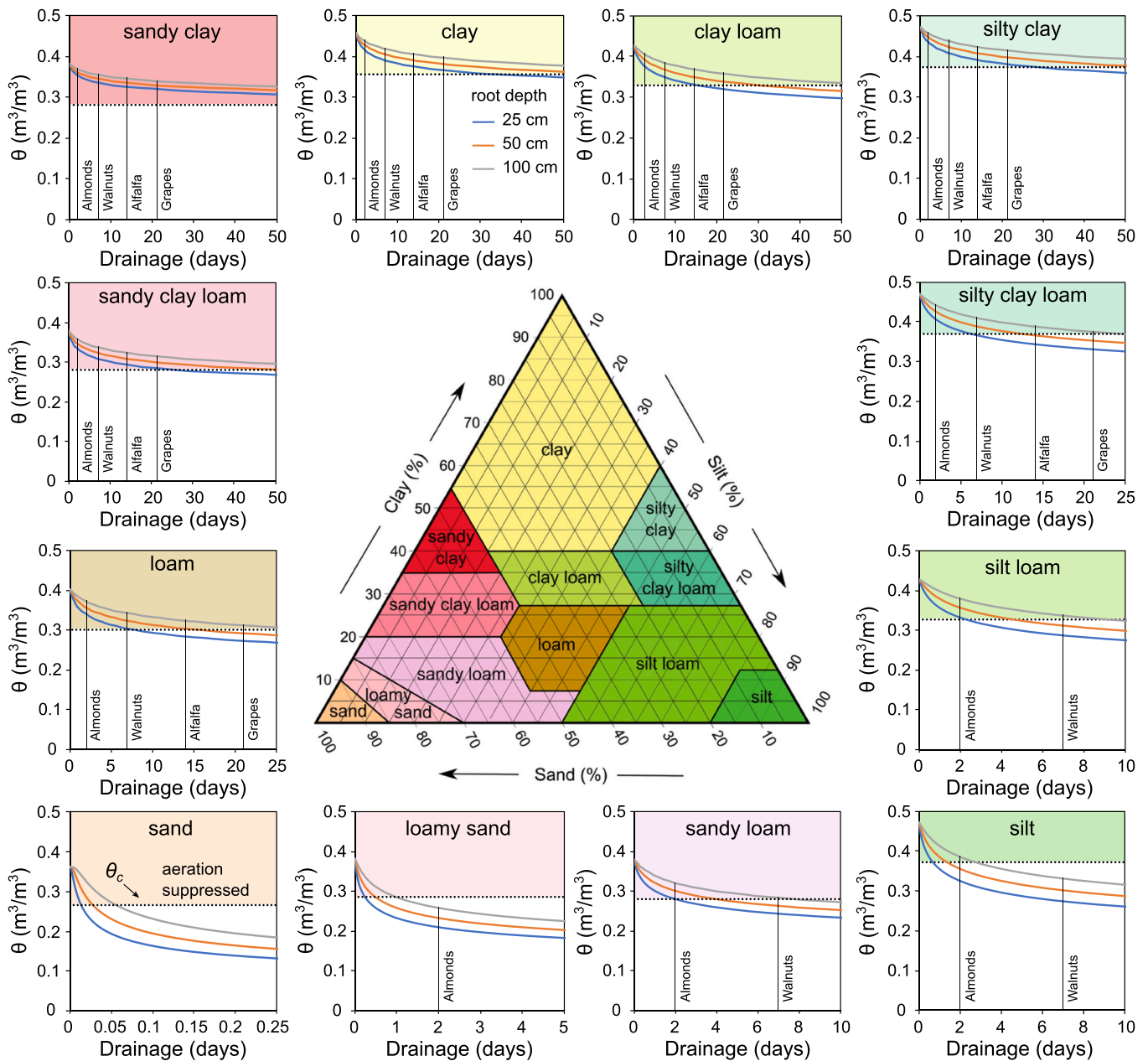
Fig. 4. Drainage curves at depths of 25, 50, and 100 cm for the USDA soil texture classes. The colored area represents conditions above the critical water content ($\theta_c = \theta_s - 0.1$) where soil aeration is suppressed. The white area below θ_c represents well-aerated root-zone conditions. Almond, walnut, alfalfa, and grape with flooding tolerance of 2, 7, 14, and 21 days, respectively, represent the four tolerance classes (see Table 3 for more details). (For interpretation of the references to colour in this figure legend, the reader is referred to the web version of this article.)

with (up to 0.054 difference in this study for the same soil and set of hydraulic parameters; Table 1). Moreover, the concept of a constant θ_c is an oversimplification used in the model, because θ_c is a function of biotic and abiotic parameters, which vary spatially and temporally for a specific soil texture. Indeed, our data indicate that during intervals of Ag-MAR flooding and drainage, different θ_c can be obtained even for the same location in the soil (data not shown). This is probably related to changes in soil respiration after flooding is initiated (Oikawa et al., 2014; Or et al., 2007) as well as SWRC hysteresis (Beriozkin and Mualem, 2018; Hannes et al., 2016).

4. Conclusions

In this study, a simple root zone residence time (RZRT) model is proposed to predict water application duration for agricultural managed

aquifer recharge (Ag-MAR) using hydraulic parameters deduced from soil texture, crop tolerance to saturation, effective root depth, and the critical water content. The results of the RZRT model show that the average error of Ag-MAR flood duration is less than 5 h and up to a few days, using fitted and unfitted parameters, respectively. For sensitive crops, it is recommended to use the model with fitted hydraulic parameters (obtained from the specific Ag-MAR site), which reduces the model error. The model can also be used as a first approximation to determine the total amount of water that could be applied during an Ag-MAR event. Ag-MAR water application duration can be quickly calculated using the RZRT learning tool, an MS Excel workbook that includes the model, hydraulic parameters, and crop properties (see Supplement Materials). The proposed model can be easily integrated into various Ag-MAR models and assessment tools.

Declaration of Competing Interest

The authors declare that they have no known competing financial interests or personal relationships that could have appeared to influence the work reported in this paper.

Acknowledgments

Appendix A. Supporting information

Supplementary data associated with this article can be found in the online version at doi:10.1016/j.agwat.2021.107031.

References

Ahuja, L.R., Barnes, B.B., Cassel, D.K., Bruce, R.R., Nofziger, D.L., 1988. Effect of assumed unit gradient during drainage on the determination of unsaturated hydraulic conductivity and infiltration parameters. Soil Sci. 145, 235–243.

Allen, R.G., Pereira, L.S., Raes, D., Smith, M., 1998. FAO Irrigation and drainage paper No. 56, Rome Food Agric. Organ. U. N. 56, e156.

Amato, M., Basso, B., Celano, G., Bitella, G., Morelli, G., Rossi, R., 2008. In situ detection of tree root distribution and biomass by multi-electrode resistivity imaging. Tree Physiol. 28, 1441–1448. https://doi.org/10.1093/treephys/28.10.1441.

Andersen, P.C., 1994. Temperate nut species. In: Schaffer, B., Andersen, P.C. (Eds.), Handbook of Environmental Physiology of Fruit Crops, Volume I, Temperate Crops. CRC Press, pp. 299–338.

Angulo-Jaramillo, R., Bagarello, V., Di Prima, S., Gosset, A., Iovino, M., Lassabatere, L., 2019. Beerkan Estimation of Soil Transfer parameters (BEST) across soils and scales. J. Hydrol. 576, 239–261. https://doi.org/10.1016/j.jhydrol.2019.06.007.

Assouline, S., Or, D., 2014. The concept of field capacity revisited: defining intrinsic static and dynamic criteria for soil internal drainage dynamics. Water Resour. Res. 50, 4787–4802. https://doi.org/10.1002/2014WR015475.

Atkinson, D., 1983. The growth, activity and distribution of the fruit tree root system. Plant Soil 71, 23–35.

Bachand, P.A.M., Roy, S.B., Choperena, J., Cameron, D., Horwath, W.R., 2014. Implications of using on-farm flood flow capture to recharge groundwater and mitigate flood risks along the Kings River, CA. Environ. Sci. Technol. 48, 13601–13609. https://doi.org/10.1021/es501115c.

Bachand, S.M., R. Hossner, and P.A.M. Bachand. 2019. Effects on soil hydrology and salinity, and potential implications on soil oxygen, Bachand & Associates, Final 2017 OFR Comprehensive Report: 38.

Barta, A.L., 1988. Response of field grown alfalfa to root waterlogging and shoot removal. I. Plant injury and carbohydrate and mineral content of roots. Agron. J. 80, 889–892. https://doi.org/10.2134/agronj1988.00021962008000060010x.

Bassoi, L.H., Hopmans, J.W., Jorge, L.A., de, C., Alencar, C.M., de, Silva, J.A.M. e, 2003. Grapevine root distribution in drip and microsprinkler irrigation. Sci. Agric. 60, 377–387. https://doi.org/10.1590/S0103-90162003000200024.

Bastani, M., Harter, T., 2019. Source area management practices as remediation tool to address groundwater nitrate pollution in drinking supply wells. J. Contam. Hydrol. 226, 103521 https://doi.org/10.1016/j.jconhyd.2019.103521.

Beckman, T., Flore, J., Perry, R., 1986. Flooding tolerance in sour cherry. Compact Fruit. Tree USA.

Ben-Noah, I., Friedman, S.P., 2018. Review and Evaluation of Root Respiration and of Natural and Agricultural Processes of Soil Aeration. Vadose Zone J. 17, 0. https://doi.org/10.2136/vzj2017.06.0119.

Beriozkin, A., Mualem, Y., 2018. Comparative analysis of the apparent saturation hysteresis approach and the domain theory of hysteresis in respect of prediction of scanning curves and air entrapment. Adv. Water Resour. 115, 253–263. https://doi.org/10.1016/j.advwatres.2018.01.016.

Bhusal, R.C., Mizutani, F., Rutto, K.L., 2002. Selection of rootstocks for flooding and drought tolerance in citrus species. Pak. J. Biol. Sci. 5, 509–512.

Bouwer, H., 1966. Rapid field measurement of air entry value and hydraulic conductivity of soil as significant parameters in flow system analysis. Water Resour. Res. 2, 729–738. https://doi.org/10.1029/WR002i004p00729.

Carr, M.K.V., 2014. The water relations and irrigation requirements of papaya (*Carica papaya* L.): a review. Exp. Agric. 50, 270–283. https://doi.org/10.1017/S0014479713000380.

Chaplin, C., Schneider, G., Martin, D., 1974. Rootstock effect on peach tree survival on a poorly drained soil. Hortscience.

Cook, F.J., Knight, J.H., 2003. Oxygen transport to plant roots: modeling for physical understanding of soil aeration. Soil Sci. Soc. Am. J. 67, 12.

Cook, F.J., Knight, J.H., Kelliher, F.M., 2013. Modelling oxygen transport in soil with plant root and microbial oxygen consumption: depth of oxygen penetration. Soil Res. 51, 539–553. https://doi.org/10.1071/SR13223.

Dahlke, H.E., Brown, A., Orloff, S., Putnam, D.H., O'Geen, T., 2018a. Managed winter flooding of alfalfa recharges groundwater with minimal crop damage. Calif. Agric. 72, 65–75.

Dahlke, H.E., LaHue, G.T., Mautner, M.R.L., Murphy, N.P., Patterson, N.K., Waterhouse, H., Yang, F., Foglia, L., 2018b. Chapter eight - managed aquifer recharge as a tool to enhance sustainable groundwater management in california: examples from field and modeling studies. In: Friesen, J., Rodríguez-Sinobas, L. (Eds.), Advances in Chemical Pollution, Environmental Management and Protection. Elsevier, pp. 215–275. https://doi.org/10.1016/bs.apmp.2018.07.003.

Dane, J.H., Hopmans, J.W., 2002. 3.3.2 Water Retention and Storage: Laboratory, in: Dane, J.H., Topp, G.C. (Eds.), Methods of Soil Analysis. ⟨https://doi.org/10.2136/sssabookser5.4.c25⟩.

Davies, F.S., Darnell, R.L., 1994. Blueberries, cranberries, and red raspberries. In: Schaffer, B., Andersen, P.C. (Eds.), Handbook of Environmental Physiology of Fruit Crops, Volume I, Temperate Crops. CRC Press, pp. 43–84.

Dokoozlian, N.K., Petrucci, V.E., Ayars, J.E., Clary, C.D., Schoneman, R.A., 1987. Artificial ground water recharge by flooding during grapevine dormancy. JAWRA J. Am. Water Resour. Assoc. 23, 307–311. https://doi.org/10.1111/j.1752-1688.1987.tb00809.x.

Duan, Z.P., Gan, Y.W., Wang, B.J., Hao, X.D., Xu, W.L., Zhang, W., Li, L.H., 2019. Interspecific interaction alters root morphology in young walnut/wheat agroforestry systems in northwest China. Agrofor. Syst. 93, 419–434. https://doi.org/10.1007/s10457-017-0133-2.

Eching, S.O., Hopmans, J.W., 1993. Optimization of hydraulic functions from transient outflow and soil water pressure data. Soil Sci. Soc. Am. J. 57, 1167–1175. https://doi.org/10.2136/sssaj1993.03615995005700050001x.

Fan, J., McConkey, B., Wang, H., Janzen, H., 2016. Root distribution by depth for temperate agricultural crops. Field Crops Res. 189, 68–74. https://doi.org/10.1016/j.fcr.2016.02.013.

Faunt, C.C., Sneed, M., Traum, J., Brandt, J.T., 2016. Water availability and land subsidence in the Central Valley, California, USA. Hydrogeol. J. 24, 675–684. https://doi.org/10.1007/s10040-015-1339-x.

Flores-Lopez, F., Arrate, D., Ceyhan, S., Bergfeld, L., 2019. Simulation of agricultural crops' root zone saturation to determine acceptable recharge duration and dry-down intervals for potential managed aquifer recharge, in: AGU Fall Meeting Abstracts, H11L-1668.

Freijer, J.I., 1994. Calibration of jointed tube model for the gas diffusion coefficient in soils. Soil Sci. Soc. Am. J. 58, 1067–1076.

Ganot, Y., Dahlke, H.E., 2021. Natural and forced soil aeration during agricultural managed aquifer recharge. Vadose Zone J. 1–19. https://doi.org/10.1002/vzj2.20128.

Gilman, E.F., 1990. Tree root growth and development. I. Form, spread, depth and periodicity. J. Environ. Hortic. 8, 215–220. https://doi.org/10.24266/0738-2898-8.4.215.

Glinski, Stepniewski, 1985. Soil Aeration and Its Role For Plants. CRC Press. https://doi.org/10.1201/9781351076685.

Grable, A.R., Siemer, E.G., 1968. Effects of bulk density, aggregate size, and soil water suction on oxygen diffusion, redox potentials, and elongation of corn roots. Soil Sci. Soc. Am. J. 32, 180–186. https://doi.org/10.2136/sssaj1968.03615995003200020011x.

Green, S.R., Clothier, B.E., 1995. Root water uptake by kiwifruit vines following partial wetting of the root zone. Plant Soil 173, 317–328. https://doi.org/10.1007/BF00011470.

Green, W.H., Ampt, G.A., 1911. Studies on soils physics: 1. The flow of air and water through soils. J. Agric. Sci. 4, 1–24.

Hamamoto, S., Moldrup, P., Kawamoto, K., Wollesen de Jonge, L., Schjønning, P., Komatsu, T., 2011. Two-region extended archie's law model for soil air permeability and gas diffusivity. Soil Sci. Soc. Am. J. 75, 795–806. https://doi.org/10.2136/sssaj2010.0207.

Hannes, M., Wollschläger, U., Wöhling, T., Vogel, H.-J., 2016. Revisiting hydraulic hysteresis based on long-term monitoring of hydraulic states in lysimeters. Water Resour. Res. 52, 3847–3865. https://doi.org/10.1002/2015WR018319.

Harter, T., 2015. California's agricultural regions gear up to actively manage groundwater use and protection. Calif. Agric. 69, 193–201.

Horn, R., Peng, X., Fleige, H., Dörner, J., 2014. Pore rigidity in structured soils—only a theoretical boundary condition for hydraulic properties? Soil Sci. Plant Nutr. 60, 3–14. https://doi.org/10.1080/00380768.2014.886159.

Hruska, J., Čermák, J., Šustek, S., 1999. Mapping tree root systems with ground-penetrating radar. Tree Physiol. 19, 125–130. https://doi.org/10.1093/treephys/19.2.125.

Hunt, A.G., 2004. Continuum percolation theory for water retention and hydraulic conductivity of fractal soils: estimation of the critical volume fraction for percolation. Adv. Water Resour. 27, 175–183. https://doi.org/10.1016/j.advwatres.2003.10.004.

Hunt, A.G., 2005. Continuum percolation theory for saturation dependence of air permeability. Vadose Zone J. 4, 134–138. https://doi.org/10.2136/vzj2005.0134a.

Insausti, P., Gorjón, S., 2013. Floods affect physiological and growth variables of peach trees (Prunus persica (L.) Batsch), as well as the postharvest behavior of fruits. Sci. Hortic. 152, 56–60. https://doi.org/10.1016/j.scienta.2013.01.005.

Kallestad, J.C., Sammis, T.W., Mexal, J.G., Gutschick, V., 2007. The impact of prolonged flood-irrigation on leaf gas exchange in mature pecans in an orchard setting. Int. J. Plant Prod. 16.

Kallestad, J.C., Sammis, T.W., Mexal, J.G., 2008a. Extent and duration of gas-phase soil oxygen depletion in response to flood-irrigations in two pecan orchards. Appl. Eng. Agric.

Kallestad, J.C., Sammis, T.W., Mexal, J.G., 2008b. Comparison of galvanic and chemiluminescent sensors for detecting soil air oxygen in flood-irrigated pecans. Soil Sci. Soc. Am. J. 72, 758–766. https://doi.org/10.2136/sssaj2007.0170.

Kocis, T.N., Dahlke, H.E., 2017. Availability of high-magnitude streamflow for groundwater banking in the Central Valley, California. Environ. Res. Lett. 12, 084009 https://doi.org/10.1088/1748-9326/aa7b1b.

Koumanov, K.S., Hopmans, J.W., Schwankl, L.W., 2006. Spatial and temporal distribution of root water uptake of an almond tree under microsprinkler irrigation. Irrig. Sci. 24, 267. https://doi.org/10.1007/s00271-005-0027-3.

Kozlowski, T.T., 1997. Responses of woody plants to flooding and salinity. Tree Physiol. 17 https://doi.org/10.1093/treephys/17.7.490 (490–490).

Lasko, A.N., 1994. Apple. In: Schaffer, B., Andersen, P.C. (Eds.), Handbook of Environmental Physiology of Fruit Crops, Volume I, Temperate Crops. CRC Press, pp. 3–42.

Lassabatère, L., Angulo-Jaramillo, R., Ugalde, J. M. Soria, Cuenca, R., Braud, I., Haverkamp, R., 2006. Soil Science Society of America Journal 70 (2), 521–532. https://doi.org/10.2136/sssaj2005.0026.

Lax, P.D., 1972. The formation and decay of shock waves. Am. Math. Mon. 79, 227–241. https://doi.org/10.2307/2316618.

Lehmann, J., 2003. Subsoil root activity in tree-based cropping systems, in: Abe, J. (Ed.), Roots: The Dynamic Interface between Plants and the Earth: The 6th Symposium of the International Society of Root Research, 11–15 November 2001, Nagoya, Japan, Developments in Plant and Soil Sciences. Springer Netherlands, Dordrecht, pp. 319–331. ⟨https://doi.org/10.1007/978-94-017-2923-9_31⟩.

Lopes, A., da, S., Hernandez, F.B.T., Alves Júnior, J., Oliveira, G.Q. de, 2014. Distribution of the root system of peach palm under drip irrigation. Acta Sci. Agron. 36, 317–321. https://doi.org/10.4025/actasciagron.v36i3.16281.

Ma, Y., Feng, S., Su, D., Gao, G., Huo, Z., 2010. Modeling water infiltration in a large layered soil column with a modified Green–Ampt model and HYDRUS-1D, Comput. Electron. Agric., Special issue on computer and computing technologies in agriculture 71, Supplement 1, S40–S47. ⟨https://doi.org/10.1016/j.compag.2009.07.006⟩.

Machado, B.D., Magro, M., Souza, D.S., de, Rufato, L., Kretzschmar, A.A., Machado, B.D., Magro, M., Souza, D.S., de, Rufato, L., Kretzschmar, A.A., 2018. Study on the growth and spatial distribution of the root system of different european pear cultivars on quince rootstock combinations. Rev. Bras. Frutic. 40. https://doi.org/10.1590/0100-29452018108.

Michelakis, N., Vougioucalou, E., Clapaki, G., 1993. Water use, wetted soil volume, root distribution and yield of avocado under drip irrigation. Agric. Water Manag. 24, 119–131. https://doi.org/10.1016/0378-3774(93)90003-S.

Mitchell, P.D., Goodwin, I., Jerie, P.H., 1994. Pear and quince, in: Schaffer, B., Andersen, P.C. (Eds.), Handbook of Environmental Physiology of Fruit Crops, Volume I, Temperate Crops. pp. 189–207.

Moldrup, P., Olesen, T., Yoshikawa, S., Komatsu, T., McDonald, A.M., Rolston, D.E., 2005. Predictive-descriptive models for gas and solute diffusion coefficients in variably saturated porous media coupled to pore-size distribution: iii. Inactive pore space interpretations of gas diffusivity. Soil Sci. 170, 14.

Mualem, Y., 1976. A new model for predicting the hydraulic conductivity of unsaturated porous media. Water Resour. Res. 12, 513–522. https://doi.org/10.1029/WR012i003p00513.

Mukhtar, S., Baker, J.L., Kanwar, R.S., 1996. Effect of short-term flooding and drainage on soil oxygenation. Trans. ASAE 39, 915–920. https://doi.org/10.13031/2013.27576.

Nasta, P., Romano, N., 2016. Use of a flux-based field capacity criterion to identify effective hydraulic parameters of layered soil profiles subjected to synthetic drainage experiments. Water Resour. Res. 52, 566–584. https://doi.org/10.1002/2015WR016979.

National Cooperative Soil Survey, 2020. National Cooperative Soil Survey Soil Characterization Database, ⟨http://ncsslabdatamart.sc.egov.usda.gov/⟩ (Accessed Monday, December 14, 2020).

Nethsinghe, D.A., Broeshart, H., 1975. Root activity patterns of some tree crops: results of a five-year coordinated research programme of the Joint FAO/IAEA Division of Atomic Energy in Food and Agriculture, Technical reports series - IAEA. International Atomic Energy Agency, Vienna.

Nimmo, J.R., Schmidt, K.M., Perkins, K.S., Stock, J.D., 2009. Rapid measurement of field-saturated hydraulic conductivity for areal characterization. Vadose Zone J. 8, 142–149. https://doi.org/10.2136/vzj2007.0159.

O'Geen, A., Walkinshaw, M., Beaudette, D., 2017. SoilWeb: a multifaceted interface to soil survey information. Soil Sci. Soc. Am. J. 81, 853–862. https://doi.org/10.2136/sssaj2016.11.0386n.

O'Geen, A.T., Saal, M., Dahlke, H., Doll, D., Elkins, R., Fulton, A., Fogg, G., Harter, T., Hopmans, J.W., Ingels, C., Niederholzer, F., Solis, S.S., Verdegaal, P., Walkinshaw, M., 2015. Soil suitability index identifies potential areas for groundwater banking on agricultural lands. Calif. Agric. 69, 75–84. https://doi.org/10.3733/ca.v069n02p75.

Oikawa, P.Y., Grantz, D.A., Chatterjee, A., Eberwein, J.E., Allsman, L.A., Jenerette, G.D., 2014. Unifying soil respiration pulses, inhibition, and temperature hysteresis through dynamics of labile soil carbon and O2. J. Geophys. Res. Biogeosci. 119, 521–536. https://doi.org/10.1002/2013JG002434.

Or, D., Smets, B.F., Wraith, J.M., Dechesne, A., Friedman, S.P., 2007. Physical constraints affecting bacterial habitats and activity in unsaturated porous media – a review. Adv. Water Resour., Biological processes in porous media: From the pore scale to the field 30, 1505–1527. ⟨https://doi.org/10.1016/j.advwatres.2006.05.025⟩.

Paltineanu, C., Nicolae, S., Militaru, M., Butac, M., Chitu, E., Tanasescu, N., Calinescu, M., Coman, R., 2017a. Spatial distribution of roots in medium-textured soils in the case of cherry trees grafted on Gi Sel A5 rootstock. Sci. Hortic. 217, 48–54. https://doi.org/10.1016/j.scienta.2017.01.033.

Paltineanu, C., Nicolae, S., Tanasescu, N., Chitu, E., Ancu, S., 2017b. Investigating root density of plum and apple trees grafted on low-vigor rootstocks to improve orchard management. Erwerbs Obstbau 59, 29–37. https://doi.org/10.1007/s10341-016-0293-7.

Oliveira, M.R.G, van Noordwijk, M., Gaze, S.R., Brouwer, G., Bona, S., Mosca, G., Hairiah, K., 2000. Auger sampling, ingrowth cores and pinboard methods. In: Smit, A.L., Bengough, A.G., Engels, C., van Noordwijk, M., Pellerin, S., van de Geijn, S.C. (Eds.), Root Methods: A Handbook. Springer, Berlin, Heidelberg, pp. 175–210.

Paltineanu, C., Coman, M., Nicolae, S., Ancu, I., Calinescu, M., Sturzeanu, M., Chitu, E., Ciucu, M., Nicola, C., 2018. Root system distribution of highbush blueberry crops of various ages in medium-textured soils. Erwerbs Obstbau 60, 187–193. https://doi.org/10.1007/s10341-017-0357-3.

Panigrahi, P., Srivastava, A.K., 2016. Effective management of irrigation water in citrus orchards under a water scarce hot sub-humid region. Sci. Hortic. 210, 6–13. https://doi.org/10.1016/j.scienta.2016.07.008.

Philip, J.R., 1992. Falling head ponded infiltration. Water Resour. Res. 28, 2147–2148. https://doi.org/10.1029/92WR00704.

Reynolds, W.D., Elrick, D.E., Youngs, E.G., Amoozegar, A., Booltink, H.W.G., Bouma, J., 2002. 3.4.3 Saturated and field-saturated water flow parameters, Dane, J.H., Clarke Topp, G., (Eds.), in: Methods of Soil Analysis. ⟨https://doi.org/10.2136/sssabookser5.4.c32⟩.

Ruiz-Sánchez, M.C., Plana, V., Ortuño, M.F., Tapia, L.M., Abrisqueta, J.M., 2005. Spatial root distribution of apricot trees in different soil tillage practices. Plant Soil 272, 211–221. https://doi.org/10.1007/s11104-004-4781-4.

Sandler, H., DeMoranville, C., Lampinen, B., 2004. Cranberry irrigation management, Cranberry Stn. Fact Sheets.

Schaffer, B., Andersen, P.C., Ploetz, R., 1992. Responses of Fruit Crops to Flooding. Horticultural Reviews, 13. John Wiley & Sons, pp. 257–313.

Selker, J.S., Assouline, S., 2017. An explicit, parsimonious, and accurate estimate for ponded infiltration into soils using the Green and Ampt approach. Water Resour. Res. 53, 7481–7487. https://doi.org/10.1002/2017WR021020.

Silva, A.P., da, Kay, B.D., Perfect, E., 1994. Characterization of the least limiting water range of soils. Soil Sci. Soc. Am. J. 58, 1775–1781. https://doi.org/10.2136/sssaj1994.03615995005800060028x.

Šimůnek, J., van Genuchten, M.T., Sejna, M., Saito, H., Sakai, M., 2009. HYDRUS-1D technical manual.

Sisson, J.B., Van Genuchten, M.T., 1991. An improved analysis of gravity drainage experiments for estimating the unsaturated soil hydraulic functions. Water Resour. Res. 27, 569–575. https://doi.org/10.1029/91WR00184.

Sisson, J.B., Ferguson, A.H., Genuchten, M.T. van, 1980. Simple method for predicting drainage from field plots. Soil Sci. Soc. Am. J. 44, 1147–1152. https://doi.org/10.2136/sssaj1980.03615995004400060004x.

Smith, G.S., Buwalda, J.G., 1994. Kiwifruit. In: Schaffer, B., Andersen, P.C. (Eds.), Handbook of Environmental Physiology of Fruit Crops, Volume I, Temperate Crops. CRC Press, pp. 299–338.

Sokalska, D.I., Haman, D.Z., Szewczuk, A., Sobota, J., Dereń, D., 2009. Spatial root distribution of mature apple trees under drip irrigation system. Agric. Water Manag. 96, 917–924. https://doi.org/10.1016/j.agwat.2008.12.003.

Thompson, T.E., Fick, G.W., 1981. Growth response of alfalfa to duration of soil flooding and to temperature. Agron. J. 73, 329–332. https://doi.org/10.2134/agronj1981.00021962007300020020x.

Topp, C.G. and Ferré, T.P.A., 2002. 3.1 Water content, in: Dane, J.H., Topp, G.C. (Eds.), Methods of Soil Analysis. ⟨https://doi.org/10.2136/sssabookser5.4.c19⟩.

Troeh, F.R., Jabro, J.D., Kirkham, D., 1982. Gaseous diffusion equations for porous materials. Geoderma 27, 239–253. https://doi.org/10.1016/0016-7061(82)90033-7.

USDA, 2007. Vegetables usual planting and harvesting dates. Agricultural Handbook Number 507. USDA National Agricultural Statistics Services, USDA, Washington, DC.

USDA, 2010. Field crops usual planting and harvesting dates. Agricultural Handbook Number 628. USDA National Agricultural Statistics Services, USDA, Washington, DC.

van Genuchten, M.Th., 1980. A closed-form equation for predicting the hydraulic conductivity of unsaturated soils. Soil Sci. Soc. Am. J. 44, 892. https://doi.org/10.2136/sssaj1980.03615995004400050002x.

van Noordwijk, M., Brouwer, G., Meijboom, F., do Rosário, G., Oliveira, M., Bengough, A. G., 2000. Trench profile techniques and core break methods. In: Smit, A.L., Bengough, A., Glyn, Engels, C., van Noordwijk, M., Pellerin, S., van de Geijn, S.C. (Eds.), Root Methods: A Handbook. Springer, Berlin, Heidelberg, pp. 211–233. https://doi.org/10.1007/978-3-662-04188-8_7.

Wang, L., Wu, W., Xiao, J., Huang, Q., Hu, Y., 2020. Effects of different drip irrigation modes on water use efficiency of pear trees in Northern China. Agric. Water Manag., 106660 https://doi.org/10.1016/j.agwat.2020.106660.

Waterhouse, H., Bachand, S., Mountjoy, D., Choperena, J., Bachand, P., Dahlke, H., Horwath, W., 2020. Agricultural managed aquifer recharge — water quality factors to consider. Calif. Agric. 74, 144–154.

Wesseling, J., Van Wijk, W., 1957. Soil physical conditions in relation to drain depth, Drain. Agric. Lands Am. Soc. Agron, Madison Wisconson 461–504.

Zhang, Y., Schaap, M.G., 2017. Weighted recalibration of the Rosetta pedotransfer model with improved estimates of hydraulic parameter distributions and summary statistics (Rosetta3). J. Hydrol. 547, 39–53. https://doi.org/10.1016/j.jhydrol.2017.01.004.

Zhang, Z.B., Peng, X., Wang, L.L., Zhao, Q.G., Lin, H., 2013. Temporal changes in shrinkage behavior of two paddy soils under alternative flooding and drying cycles and its consequence on percolation. Geoderma 192, 12–20. https://doi.org/10.1016/j.geoderma.2012.08.009.